Annals of Hepatology 30 (2025) 101744

Contents lists available at ScienceDirect

Annals of Hepatology

journal homepage: www.elsevier.es/annalsofhepatology

Original article

Integrated analyses and a novel nomogram for the prediction of significant fibrosis in patients

Mengxin Lu[a,1], Shuai Tao[b,1], Xinyan Li[a,1], Qunling Yang[a], Cong Du[a], Weijia Lin[c], Shuangshuang Sun[d], Conglin Zhao[a], Neng Wang[a], Qiankun Hu[a], Yuxian Huang[a], Qiang Li[a,*], Yi Zhang[a,*], Liang Chen[a,*]

[a] Department of Liver Disease, Shanghai Public Health Clinical Center, Fudan University, Shanghai, China
[b] Scientific Research Center, Shanghai Public Health Clinical Center, Fudan University, Shanghai, China
[c] Department of Hepatobiliary Medicine, Shanghai Public Health Clinical Center, Fudan University, Shanghai, China
[d] Department of liver disease center, Shanghai Public Health Clinical Center, Fudan University, Shanghai, China

ARTICLE INFO

Article History:
Received 10 April 2024
Accepted 23 August 2024
Available online 29 November 2024

Keywords:
Liver fibrosis
LTBP2
Nomogram
Biomarker

ABSTRACT

Introduction and Objectives: This study aimed to explore the key genes involved in the pathophysiological process of liver fibrosis and develop a novel predictive model for noninvasive assessment of significant liver fibrosis patients.

Patients and Methods: Differentially expressed genes (DEGs) were identified using the Limma package. The hub genes were explored using the CytoHubba plugin app and validated in GEO datasets and cell models. Furthermore, serum LTBP2 was measured in liver fibrosis (LF) patients with biopsy-proven by ELISA. All patients' clinical characteristics and laboratory results were analyzed. Finally, multivariate logistic regression analysis was used to construct the model for visualization by nomogram. Area under the receiver operating characteristic curve (AUROC) analysis, calibration curves, and decision curve analysis (DCA) certify the accuracy of the nomogram.

Results: RNA sequencing was performed on the liver tissues of 66 biopsy-proven HBV-LF patients. After multiple analyses and in vitro simulation of HSC activation, LTBP2 was found to be the most associated with HSC activation regardless of the causes. Serum LTBP2 expression was measured in 151 patients with biopsy, and LTBP2 was found to increase in parallel with the fibrosis stage. Multivariate logistic regression analysis showed that LTBP2, PLT and AST levels were demonstrated as the independent prediction factors. A nomogram that included the three factors was tabled to evaluate the probability of significant fibrosis occurrence. The AUROC of the nomogram model was 0.8690 in significant fibrosis diagnosis.

Conclusions: LTBP2 may be a new biomarker for liver fibrosis patients. The nomogram showed better diagnostic performance in patients.

Abbreviations: α-SMA, α-Smooth muscle actin; ALT, Alanine aminotransferase; ALB, Albumin; ALP, Alkaline Phosphatase; apoA1, Apolipoprotein A1; apoB, Apolipoprotein B; AST, Aspartate aminotransferase; AUROC, Area under receiver operating characteristic curve; BP, Biological processes; CC, Cellular components; DBIL, Direct Bilirubin; DCA, Decision curve analysis; DEGs, Differentially expressed genes; DMNC, Density of Maximum Neighborhood Component; ECM, Extracellular matrix; EPC, Edge Percolated Component; GGT, Gamma-Glutamyl Transferase; GLU, Glucose; HBV, Hepatitis B Virus; HCT, Hematocrit; HGB, Hemoglobin; HDL-C, High-Density Lipoprotein Cholesterol; HSCs, Hepatic Stellate Cells; INR, International Normalized Ratio; KEGG, Kyoto Encyclopedia of Genes and Genomes; LF, Liver fibrosis; LDH, Lactate Dehydrogenase; LTBP2, Latent transforming growth factor beta binding protein 2; MCHC, Mean Corpuscular Hemoglobin Concentration; MCC, Maximal Clique Centrality; MF, Molecular functions; MNC, Maximum Neighborhood Component; MPV, Mean Platelet Volume; NSF, Non-significant fibrosis; PA, Prealbumin; PPI, Protein-protein interaction; PLT, Platelet Count; PT, Prothrombin Time; RBC, Red blood cell; RDW-CV, Red Cell Distribution Width-Coefficient of Variation; SF, Significant fibrosis; Tbil, Total bilirubin; TC, Total Cholesterol; TP, Total Protein; TG, Triglycerides; WBC, White blood cell

* Corresponding authors.
E-mail addresses: lumxxin@foxmail.com (M. Lu), taoshuai@shaphc.org (S. Tao), lixinyan@shaphc.org (X. Li), 21211300005@m.fudan.edu.cn (Q. Yang), 18883939727@163.com (C. Du), linweijia@shaphc.org (W. Lin), 13818680249@163.com (S. Sun), lin15993001733@163.com (C. Zhao), 2277466396@qq.com (N. Wang), huqiankun168@163.com (Q. Hu), yxhuang@fudan.edu.cn (Y. Huang), liqiang66601@163.com (Q. Li), zhangyi117@shaphc.org (Y. Zhang), chenliang@shaphc.org (L. Chen).

[1] Mengxin Lu, Shuai Tao and Xinyan Li are co-first authors; they contributed equally to the work.

https://doi.org/10.1016/j.aohep.2024.101744

1. Introduction

Liver fibrosis (LF) is a pathological repair response of the liver to chronic liver injury caused by various factors. It is manifested by increased extracellular matrix (ECM) production and reduced degradation, leading to diffuse excessive deposition and abnormal distribution in the liver [1]. LF involves complex interactions between multiple lineages of non-hematopoietic cells, with hepatic stellate cells (HSCs) being the most important [2]. They are the primary sources of ECM secretion and play a vital role in the occurrence and development [3]. Normally HSCs are located in the Disse gap, where they are at rest and store vitamin A. However, HSCs transform into myofibroblasts in response to injury, begin to express α-smooth muscle actin (α-SMA), migrate to tissue repair sites, and secrete large amounts of ECM [4].

The causes of LF include viral infection, drug toxicity, and fatty liver. Studies have shown that the severity of fibrosis is closely related to adverse liver outcomes [5]. Despite treatment with antiviral drugs, 7.2 % of patients with chronic HBV infection have advanced LF compared to 2.9 % of controls without hepatitis B infection [6]. HBV-related mortality remains a major problem due to the high prevalence of hepatitis B. Besides viral hepatitis, fatty liver disease, alcohol-induced LF, and cirrhosis should not be ignored. At present, the treatment for liver fibrosis mainly includes etiological treatment and anti-fibrosis treatment, but there are no specific anti-liver fibrosis drugs in clinical practice. Hence, it is critical to identify patients at high risk for significant fibrosis regardless of the causes and seek a new target.

Additionally, LF staging depends on liver biopsy, which is an invasive procedure with some risks for patients [7]. First of all, the patient's acceptance is low; there is a risk of bleeding, perforation, and other complications, and he needs to be hospitalized during the puncture examination. Secondly, it is easy to be limited by the technology and experience of operators and pathologic film readers [8]. A variety of non-invasive tools are already available to assess the stage of liver fibrosis and monitor its progression. Transient elastography (TE) is a safe and non-invasive method to estimate the degree of liver fibrosis by detecting the elastic value of the liver [9]. However, obesity, stenosis of the costal space, extrahepatic cholestasis, and ascites may increase the rate of operation failure and affect the interpretation of the fibrosis degree. In contrast, the use of serum biomarkers for evaluation has many advantages, such as easy sample collection, low risk to patients, and repeatability of the test. Direct serum markers [9], such as hyaluronic acid, type III procollagen peptide, type IV collagen, laminin, etc., can be easily and repeatable for follow-up. However, the results exhibit a relatively low correlation with the pathological stages of liver fibrosis, along with low accuracy and specificity. Additionally, there is still a dearth of a unified diagnostic threshold for clinical application. And a variety of serum indexes of another joint diagnosis of liver fibrosis score models such as Aspartate aminotransferase and Platelet ratio index (Aspartate aminotransferase to Platelet Ratio Index, APRI), The Fibrosis Index Based on 4 Factors (FIB-4) has not yet reached a consensus. A study of HBV-infected people in China showed that APRI and FIB-4 were not relatively effective in the diagnosis of liver fibrosis and cirrhosis, and the non-invasive model was more suitable for HBeAg-positive patients than HBeAg-negative patients [10]. Therefore, there is an urgent need to develop new alternative non-invasive biomarkers to identify patients with significant liver fibrosis.

Data mining has been applied in many fields, and bioinformatics analysis can help identify differentially expressed genes and molecular mechanisms. Liver tissue transcriptome analysis of fibrosis patients has been performed to fully understand the molecular abnormalities involved in their disease progression. However, the discovery of omics-based biomarkers has not been fully utilized. In this study, we sequenced 66 liver tissue samples from patients with HBV-LF, analyzed the differential genes in different fibrosis stages using bioinformatics, and combined it with human HSCs sequencing to find the factors related to LF development. Then, we focused on Latent transforming growth factor β binding protein 2 (LTBP2) and evaluated the viability of LTBP2 as a new biomarker using serum from 151 patients who underwent liver biopsy. The study overview is in Supplementary Fig. 1.

2. Patients and Methods

2.1. Liver fibrosis patients

Liver biopsy samples from 66 naive HBV-infected patients were obtained. Among the recruited patients, patients were admitted to the Shanghai Public Health Clinical Center affiliated with Fudan University. All patients were diagnosed based on the criteria recommended by the Asian Pacific Association for the Study of the Liver (APASL) [11] and had not previously received antiviral therapy.

A total of 151 serum samples were collected from patients undergoing liver biopsy at the Shanghai Public Health Clinical Center affiliated with Fudan University. Clinical data and laboratory examination were obtained using standard data collection forms from electronic medical records.

All the samples were sent to the Pathology Department of Shanghai Public Health Clinical Center, affiliated with Fudan University, for histopathology diagnosis. The stages of fibrosis (Scheuer S) and inflammation (Scheuer G) were interpreted independently by two experienced pathologists [12,13]. According to the guidelines for diagnosing and treating liver fibrosis, S0-1 indicates non-significant fibrosis (NSF), while Scheuer $\geq$ S2 is defined as significant fibrosis (SF) [14].

2.2. Enzyme-linked immunosorbent assay

The serum samples were kept in $a-80$ °C freezer until measurements. Serum LTBP2 levels were examined with the ELISA (ELK Biotechnology, Wuhan, China) kit following the manufacturer's protocols.

2.3. Traditional noninvasive fibrosis diagnostic model

APRI [15] index: APRI ={(AST/AST_{ULN})/PLT(10^9/L)} $\times$ 100
FIB-4 [16] index: FIB-4 =age $\times$ AST(U/L)/PLT(10^9/L) $\times$ ALT(U/L)$^{1/2}$

2.4. Statistical analysis

The data were processed using SPSS 25.0 and GraphPad 7.0 software and presented as the mean $\pm$ standard deviation (mean $\pm$ SD). Unless otherwise stated, categorical variables are expressed as frequency and percentage (n%), and continuous variables are expressed as median (IQR). Comparison between groups was performed by t-test, Mann Whitney U test, $\chi 2$ test, or Fisher exact test. The correlation between the two parameters was assessed using Spearman's rank-order correlation analysis. The best cut-off value is found by the Youden index. The risk factors related to patients with significant fibrosis were analyzed using univariate and multivariate logistic regression models. Based on the results of the multivariate analysis, a nomogram model was drawn using the R rms package. An analysis of the area under the receiver operating characteristic curve (AUROC) was performed on the model. The calibration curves of the training cohort and the verification cohort were adjusted after 1000 self-weightlifting samples, and the consistency of prediction probability and observation probability was analyzed. By quantifying the net benefits under different threshold probabilities, decision curve analysis (DCA) was performed to determine the clinical applicability of the

model. *P*-value < 0.05 indicated that the difference was statistically significant.

All other information on materials and methods is provided in the Supplementary Data.

2.5. Ethical statement

This study was in accordance with the ethical standards of the institutional and national research committee and with the Declaration of Helsinki (as revised in 2013). The ethics committee of Shanghai Public Health Clinical Center, Fudan University, approved this study (2023-S081-02).

3. Results

3.1. Clinical characteristics of HBV-related LF patients

Our study included 66 adult patients who were diagnosed with HBV-related liver fibrosis. There are 38 (57.6 %) males, and the average age of the whole cohort is 38.28 ± 9.8. Liver biopsy is the standard to diagnose fibrosis, and sequential histological staging of fibrosis (Scheuer score 'S') and grading of inflammation (Scheuer score 'G') can be used to assess the LF progression [17]. The numbers of patients by fibrosis stage (1/2/3/4) and inflammation grade (1/2/3) were 27/12/16/11 and 27/31/8, respectively. Virological markers, including HBV DNA, HBsAg, and HBeAg, were used to monitor viral replication and guide antiviral therapy. The four items of serum liver fibrosis also indicated the progression of fibrosis. The clinical features of each patient are listed in Supplementary Table 2.

3.2. Differential mRNA screening, GO, and pathway enrichment analysis of HBV-related LF patients

Since the liver histological Scheuer score is the most relevant fibrosis assessment, we analyzed DEGs at different stages. The volcano plots of DEGs between different groups are shown in Fig. 1A. S2 had 12 upregulated and four downregulated genes, S3 had 202 upregulated and 23 downregulated genes, and S4 had 422 upregulated and 41 downregulated genes, with stage S1 as the control (Fig. 1B). From our results, we observed that the number of upregulated DEGs among patients in stages S3 and S4 is more than in the early stage of disease progression. In addition, it can be seen that the number of downregulated DEGs associated with fibrosis also increases with the progression of the disease (Fig. 1B).

We compared the SF and NSF groups to identify key genes involved in fibrosis development. There were 1833 upregulated and

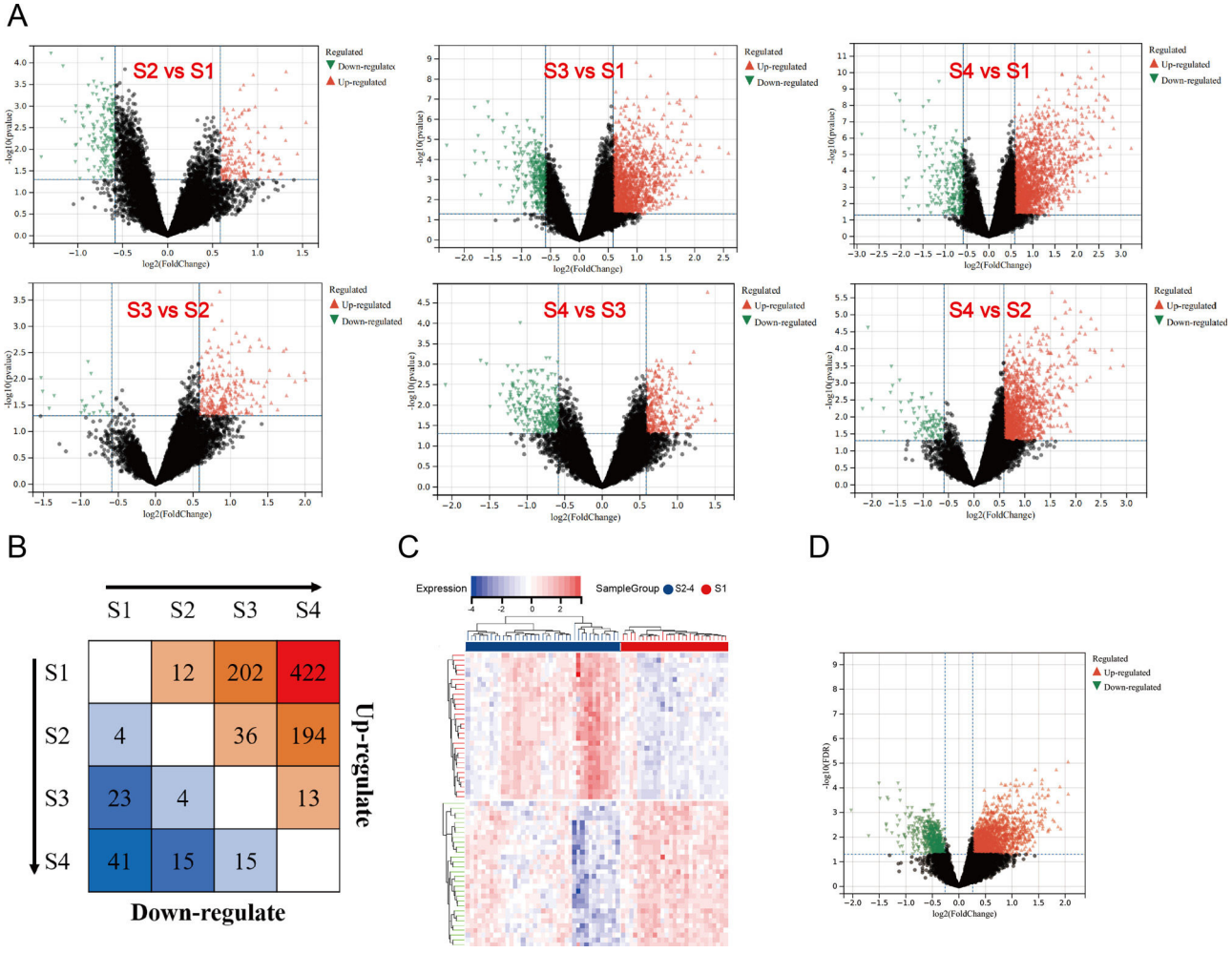

Fig. 1. The results of DEGs in different histological stages. A. Volcano plots visualizing the DEGs were analyzed among each fibrosis stage. The X-axis shows the fold change, while the Y-axis shows the *p*-value. A vertical line indicates an increase or decrease of 1.2 times. The horizontal line indicates p value = 0.05. Red dots indicate up-regulated genes, black dots indicate no significant change genes, and green dots indicate down-regulated genes. B. The number of DEGs was shown by a heatmap. The number of up-regulated genes is shown in the upper half, and down-regulated genes are shown in the lower half. C. The heatmap of DEGs among the significant fibrosis group and non-significant fibrosis group. D. The volcano plot of DEGs among the significant fibrosis group and non-significant fibrosis group. (For interpretation of the references to color in this figure legend, the reader is referred to the web version of this article.)

608 downregulated genes in SF, with NSF as a control. The heatmap and volcano plot of DEGs are shown in Fig. 1C& D.

GO and KEGG pathway enrichment analysis was employed to investigate the functions of DEGs between the SF and NSF groups. The results showed that the DEGs were enriched in 17 KEGG pathways, 212 GO-BP pathways, 16 GO-CC pathways, and 14 GO-MF pathways. We summarized the top three of each way (Supplementary Fig. 2A). ECM-receptor interaction was the most enriched pathway for DEGs. DEGs were enriched for ECM structural constituents in the MF category. DEGs were primarily enriched in collagen-containing ECM in the CC category. The DEGs were mainly enriched in ECM organization in the BP category. These results suggested that biological processes associated with fibrosis are strongly activated. The gene expression enriched into each pathway of the top five was further demonstrated in detail (Supplementary Fig. 2B and Supplementary Table 3).

3.3. PPI network construction and identification of hub genes

A PPI network for these DEGs was constructed using the search tool to retrieve interacting genes (STRING) and identify which DEGs were most probably the key genes in the LF process. A total of 127 DEGs were filtered into the PPI network complex and visualized using the Cytoscape software (Fig. 2A).

We used the CytoHubba [18] plug- in Cytoscape [19] to identify the hub genes with 12 built-in centrality indices: Maximal Clique Centrality (MCC), Density of Maximum Neighborhood Component (DMNC), Maximum Neighborhood Component (MNC), Degree, Edge Percolated Component (EPC), Bottleneck, Eccentricity, Closeness, Radiability, Betweenness, Stress and Clustering Coefficient to calculate the hub scores of significant modules. The top 30 genes in each centrality index were considered highly credible hub candidates. We applied a strict filter criterion to 12 lists of potential hub genes ranked by different hub scores. Only genes within the intersection of ≥ 6 lists were considered high-confidence hub genes with potential biological significance [20] (Fig. 2B and Supplementary Table 4). The high-confidence hub genes as follows: COL1A1, COL1A2, SPP1, TGFB2, THY1, CD248, COL3A1, COL5A1, EPCAM, ITGA3, KRT19, KRT7, LOXL1, LUM, SOX9, THBS2, AEBP1, CD24, ITGB4, LAMA1, ITGB8, LTBP2, COL15A1, COL16A1, COL4A3, COL8A2, EFEMP1, NOTCH3, WNT2B, CFTR, SPINT1.

3.4. Differential mRNA screening in the HSC-activated and validate the high-confidence hub genes

HSC activation is essential for LF progression. We analyzed the HSC transcriptome GSE68001 [21] from the GEO database to ascertain whether the dysregulated expression patterns of the identified LF-specific genes were consistent across liver tissues and HSCs. HSCs were isolated from healthy liver and culture-activated as aHSC in GSE68001. Activated HSCs had 3221 upregulated and 2180 downregulated genes compared to qHSCs (Supplementary Fig. 3). Based on these results, we used bioinformatics tools to obtain the common DEGs among GSE68001 and high-confidence hub genes in HBV-related LF. The results showed that 16 genes were upregulated, while none were downregulated. The common genes as follows: AEBP1, COL1A1, COL3A1, COL1A2, COL5A1, LOXL1, KRT7, LTBP2, COL16A1, THBS2, NOTCH3, ITGA3, THY1, LUM, CD248, EFEMP1. Spearman correlation was constructed using expression values and histological scores (Supplementary Fig. 4). Genes highly associated with disease severity ($R > 0.6$) were AEBP1, COL1A1, COL3A1, COL1A2, COL5A1, LOXL1, KRT7, LTBP2, COL16A1, THBS2 and NOTCH3.

High-confidence hub gene expression was confirmed in LX-2 cells treated with recombinant human TGF-β, and LX-2 cells expressed more α-SMA, indicating the successful establishment of the cell model. (Fig. 3A and B). Fig. 3C displays a statistical analysis of 11 high-confidence hub genes relative expression to GAPDH; eight of them were upregulated significantly. Some gene expression trends may be inconsistent due to incomplete representation of activated HSCs or gene expression in other cells, such as hepatic parenchymal and Kupffer cells.

COL1A1, COL1A2, COL5A1 and COL16A1 are key structural components where collagen family members participate in ECM. LOXL1 [22], AEBP1 [23,24] and THBS2 [25,26] have been extensively studied in LF. LTBP2, which has never been studied in LF, aroused our interest. We searched additional databases of LF caused by HBV, HCV, NAFLD and alcoholism to demonstrate further whether LTBP2 is an etiologically dependent agent of LF. We found that LTBP2 expression increased, regardless of the causes of LF (Fig. 4).

3.5. Serum LTBP2 levels identified patients with significant LF

In our transcriptome data set, LTBP2 expression levels showed stepwise up-regulation parallel to the fibrosis stage (Supplementary Fig. 4H), and the expression levels of COL1A1 and ACTA2 were strongly correlated with LTBP2 (Supplementary Fig. 5). The AUROC of intrahepatic LTBP2 mRNA levels for significant fibrosis was significantly higher than that of the FIB-4 index and APRI index (Supplementary Fig. 6). LTBP2 is a multi-domain extracellular matrix protein soluble in blood. Next, we investigated the potential of serum LTBP2 as a noninvasive biomarker to distinguish patients with SF using 151 patients with biopsy. The numbers of patients by fibrosis stage (0/1/2/3/4) and inflammation grade (0/1/2/3) were 23/69/28/18/13 and 2/99/32/18 respectively. There was no difference in age between the two groups (92 patients with NSF and 59 patients with SF), with a higher proportion of males in the SF group ($P < 0.05$) (Supplementary Table 5). Serum LTBP2 levels showed a stepwise elevation along with the fibrosis stage, and patients in the SF group are much higher than those with NSF (14.16 ng/mL vs. 8.72 ng/mL, $P < 0.0001$) with a cut-off value of 11.38 ng/mL (Fig. 5 and Supplementary Table 5).

3.6. Nomogram and validation of the model

We wanted to construct a new clinical model to predict the probability of patients developing SF. The number of patients in the training and the validation datasets was close to 7:3, as previous studies described [27]. There are 106 patients in the training cohort and 45 patients in the validation cohort. In the training cohort, we detected several differences between the NSF and the SF patients in laboratory findings, including high LTBP2 level (8.32 ng/mL vs. 13.23 ng/mL, $P < 0.0001$), lower PLT level (189.00 (10×9/L) vs. 147.00 (10×9/L), $P < 0.0001$), higher RDW-CV level (12.40 vs. 12.80, $P = 0.005$), higher AST (27.00 U/L vs. 44.00 U/L, $P = 0.0002$), lower ALB (43.80 g/L vs. 41.00 g/L, $P = 0.037$) and PA level (231.30 mg/L vs. 163.84 mg/L, $P < 0.0001$), longer PT time (13.30 s vs. 13.90 s, $P = 0.002$) and INR (1.00 vs. 1.08, $P = 0.002$) in SF group (Supplementary Table 6).

To find the factors most associated with the development of significant liver fibrosis in patients, we analyzed the laboratory parameters using univariate and multivariate analysis in this study (Table 1). In univariate analysis of the training cohort, the increased LTBP2 and AST levels, the decreased PLT and PA levels, longer PT time, and INR were associated with the development of significant fibrosis. Next, we used the data for multivariate logistic regression analysis for the factors of developing significant fibrosis (Table 1). Three variables, including serum LTBP2 levels (odds ratio 1.338, 95 % CI 1.159−1.543, $P < 0.0001$), PLT levels (0.983, 95 % CI 0.970−0.996, $P = 0.009$), and AST levels (1.010, 95 % CI 1.001−1.019, $P = 0.033$) were demonstrated as the independent prediction risk factors.

Based on the results of multiple logistic regression, we constructed a nomogram to predict the probability of SF occurrence in patients and named it the LPA model (Fig. 6). The maximum cut-off point value of the Youden index was 60 points, and the sensitivity,

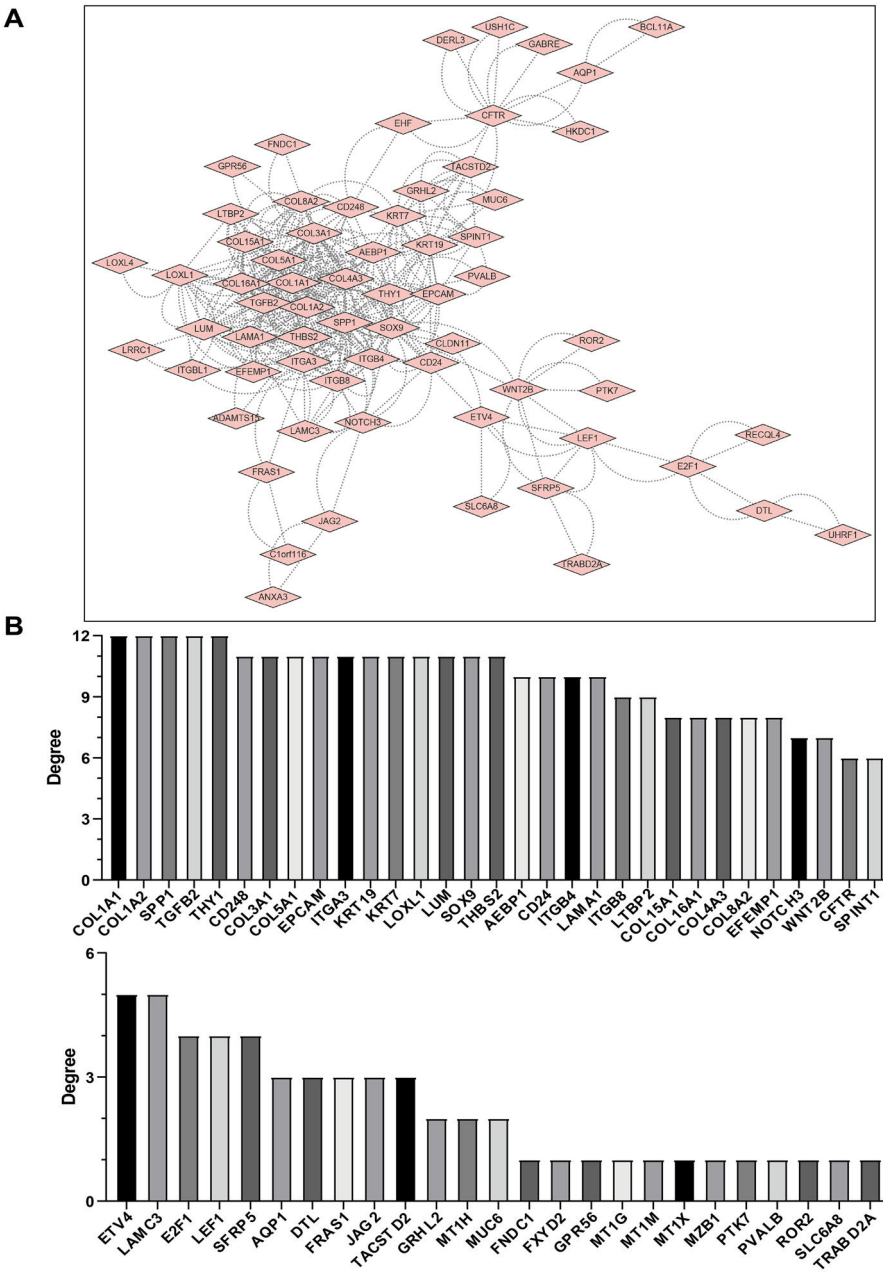

Fig. 2. PPI network analysis of DEGs with HBV-related fibrosis. A: Using the STRING online database, a total of 127 DEGs (116 up-regulated genes and 11 down-regulated genes) were screened into a DEG PPI network complex by cytoscape. Each node represents a gene, and the edges stand for the interactions between nodes (the disconnected nodes are not shown) B. Key genes were screened using CytoHubba in Cytoscape software. To ensure the reliability of the screened genes, 12 kinds of scoring (MCC, DMNC, MNC, Degree, EPC, BottleNeck, EcCentricity, Closeness, Radiality, Betweenness, Stress and ClusteringCoefficient) were used and the first 30 genes obtained from each scoring standard were selected, and then their intersection was taken to calculate the occurrence times of each gene. If a gene can appear in the list of more than 6 key genes, it is considered a key gene with high confidence.

specificity, positive predictive value, and negative predictive value of the model were 0.767, 0.873, 0.805, and 0.846, respectively. In addition, we uploaded the model to a web page for clinicians to easily use (https://model-of-lf.shinyapps.io/LPA-MODEL/).

As is shown in the nomogram, three factors bring varying degrees of risk to patients. High levels of LTBP2 bring the highest risk to patients, followed by high levels of AST and decreased PLT. An overall score scale board is listed below to calculate the likelihood of SF developing by adding the scores for the three risk factors (Fig. 6). The area under the curve (AUC) for the nomogram was 0.8690 (95 % CI: 0.7940 to 0.9439, $P < 0.0001$) (Fig. 7A). With 1000 cycles of bootstrap resampling, the calibration curve of the model indicated good agreement between the predicted probability and the observed probability (Supplementary Fig. 7A). In addition, the probability of patients' SF occurring in the validation cohort was calculated using the nomogram model. The nomogram of the validation cohort displayed an area under the curve (AUC) of 0.9152 (95 % CI: 0.8185 to 1.000, $P < 0.0001$) (Fig. 7B) with a good calibration curve in estimating the risk (Supplementary Fig. 7B). The diagnostic performance of LPA model was then compared with APRI (0.7604, 95 % CI: 0.6698 to 0.8510, $P < 0.0001$), FIB-4 (0.7608, 95 % CI: 0.6678 to 0.8538, $P < 0.0001$) and Fibroscan (0.7107, 95 % CI: 0.5930 to 0.8283, $P = 0.0017$), and the LPA model was found to have advantages (Fig. 7). APRI index includes AST and PLT. Therefore, we compared the LPA model with LTBP2 combined APRI (0.8487, 95 % CI: 0.7699 to 0.9274, $P < 0.0001$ (Fig. 7), and the results showed that the LPA model still

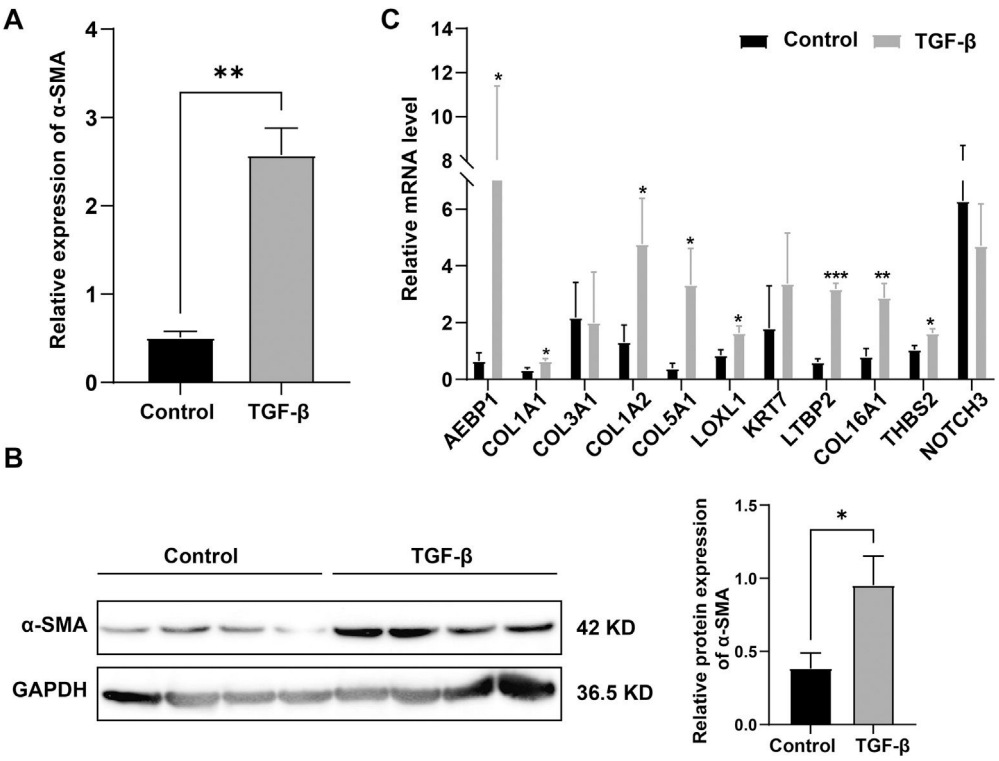

Fig. 3. Validation of the Key DEGs. A. The detection of mRNA expressions of α-SMA in the LX-2 cells by qPCR. B. Western blot detection of α-SMA in the LX-2 cells. C: The detection of mRNA expressions of 11 hub genes in cell model by qPCR.

had advantages. Decision curve analysis (DCA) further evaluates the nomogram model and shows the nomogram model presented a greater net benefit with a wider range of threshold probabilities for predicting the risk of people developing SF (Supplementary Fig. 8).

4. Discussion

In this study, we performed RNA sequencing of liver tissue from 66 naive hepatitis B patients and obtained a comprehensive analysis of molecular abnormalities associated with fibrosis development. We focused on studying gene expression profiles between SF and NSF samples and identified DEGs that could provide new insights into LF. With the NSF as a control, there are 1833 upregulated and 608 downregulated genes in significant fibrosis. Pathway analysis revealed that biological processes associated with fibrosis are highly activated, suggesting a potential application of omics approaches in identifying patients with SF. Using Cytoscape software, we have identified 31 high-confidence hub genes that may play a role in liver fibrosis.

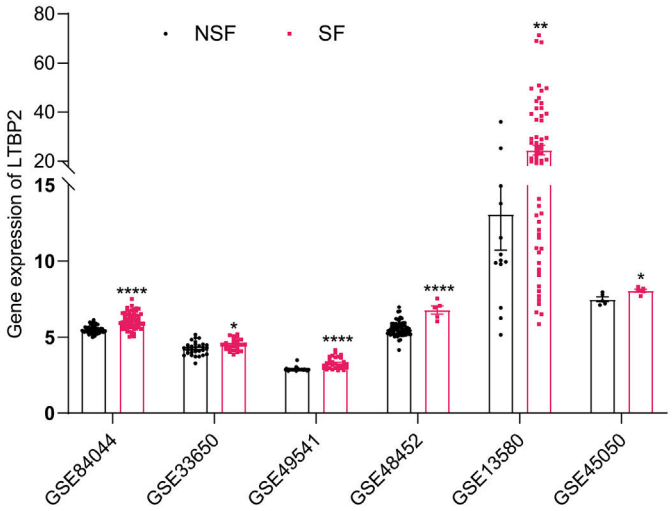

Fig. 4. The expression of LTBP2 in GEO datasets. Gene expression of LTBP2 in GSE84044, GSE33650, GSE49541, GSE48452, GSE13580 and GSE45050.

HSCs are the most important effector cells involved in hepatic fibrosis. They are the primary sources of ECM secretion and play a crucial role in the occurrence and development of liver fibrosis [3,28]. We analyzed one HSC transcriptome GSE68001, from the GEO datasets. These genes were analyzed for HSC activation, and 16 genes related to liver fibrosis and HSC activation were obtained. Spearman correlations were constructed using gene expression values and histological scores, and genes with $R > 0.6$ were considered highly associated with fibrosis. AEBP1, COL1A1, COL3A1, COL1A2, COL5A1, LOXL1, KRT7, LTBP2, COL16A1, THBS2 and NOTCH3 are considered to be the most associated with HSC activated and have priority in differentiating the stages of liver fibrosis.

When HSCs were activated in vitro with TGF-β for 24h, AEBP1, COL1A1, COL1A2, COL5A1, LOXL1, LTBP2, COL16A1 and THBS2 were significantly upregulated. COL1A1, COL1A2, COL5A1, and COL16A1 are key structural components in which members of the collagen family participate in ECM. To date, LOXL1 [22,29] and THBS2 [25,26] have been widely studied in LF. AEBP1 is a widely expressed protein in tissues rich in ECM, such as adipose tissue, large blood vessel walls, skin, and other organs [30]. Previous studies have shown that ACLP [31] is highly expressed in the lung tissues of patients with pulmonary fibrosis and mice. A study[23] has shown that miR-372-3p upregulates AEBP1 in patients with non-alcoholic steatohepatitis with worsening fibrosis, but more detailed mechanisms are lacking. Recently, research has shown that AEBP1 silencing alleviates renal fibrosis in vivo and in vitro via inhibiting the β-catenin signaling pathway [32]. Studying AEBP1's mechanism in LF could serve as a therapeutic target and biomarker. The role of LTBP2 in LF has not been

Table 1
Risk factors related to NSF and SF groups in the training cohort.

Characteristics	Univariable OR (95 %CI)	*P* value	Multivariable OR (95 %CI)	*P* value
LTBP2	1.324 (1.170–1.498)	<0.0001	1.338 (1.159–1.543)	<0.0001
PLT	0.984 (0.975–0.993)	0.0004	0.983 (0.970–0.996)	0.009
RDW-CV	1.128 (0.863–1.474)	0.378		
AST	1.009 (1.002–1.017)	0.018	1.010 (1.001–1.019)	0.033
ALB	0.933 (0.867–1.004)	0.065		
PA	0.989 (0.983–0.996)	0.001		
INR	862.302 (9.622–77,274.473)	0.003		
PT	1.926 (1.241–2.989)	0.003		

validated experimentally. In the present study, we validated a strong positive association between liver LTBP2 levels and the progression of fibrosis.

Next, we searched for other causes of liver fibrosis. Through transcriptome analysis, we identified that LTBP2 was most significantly upregulated in the livers of patients with significant fibrosis, not limited to the causes. Indeed, the intrahepatic LTBP2 level is strongly associated with fibrogenesis markers (COL1A1 and ACTA2). The AUROC of LTBP2 mRNA levels for significant fibrosis was superior to the FIB-4 index and APRI index. Subsequently, we also demonstrated the effectiveness of serum LTBP2 as a non-invasive biomarker for the identification of SF. The nomogram of the LPA model, including serum LTBP2 level, PLT, and AST was identified to predict the probability of SF occurrence in patients. The nomogram shows how the three independent predictors affect the prognosis. The AUROC for the nomogram was 0.8690 (95 % CI: 0.7940 to 0.9439, $P < 0.0001$), and validation in the validation cohort was 0.9152 (95 % CI: 0.8185 to 1.000, $P < 0.0001$). Meanwhile, we have verified the accuracy and clinical applicability of the model through calibration curves and DCA. The LPA model might provide even better diagnostic ability for significant fibrosis, and we posted the model to the web with the hope of making it available to more clinicians in the future.

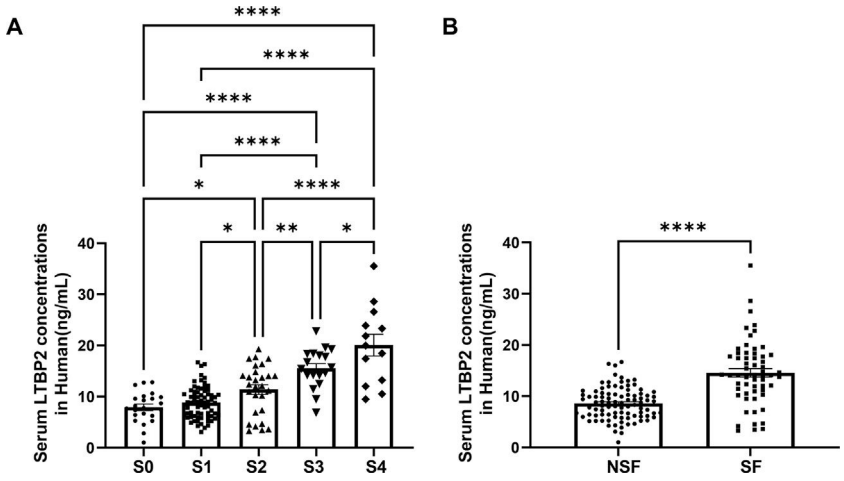

Fig. 5. Serum LTBP2 levels of 151 patients. A. Relative serum LTBP2 levels in different stages of LF patients. B. Relative serum LTBP2 levels in SF and NSF group.

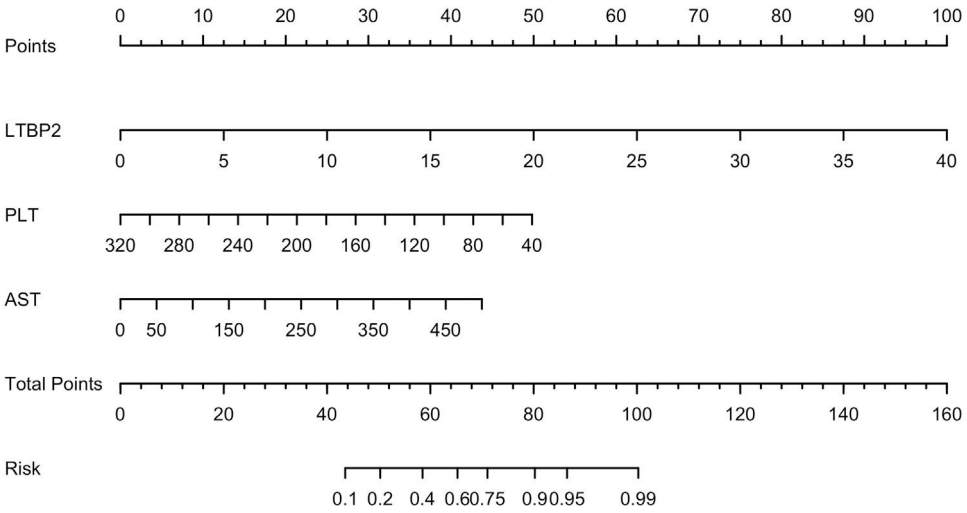

Fig. 6. The nomogram of the LPA model. A Nomogram to evaluate the risk factors for patients developing significant fibrosis. In the nomogram, all relevant patient values have been positioned and drawn up along each variable axis and a point axis to determine the score for each variable value calculation. The score of the sum is located on the total axis, and a line is drawn down to determine the probability of the patient having an adverse outcome.

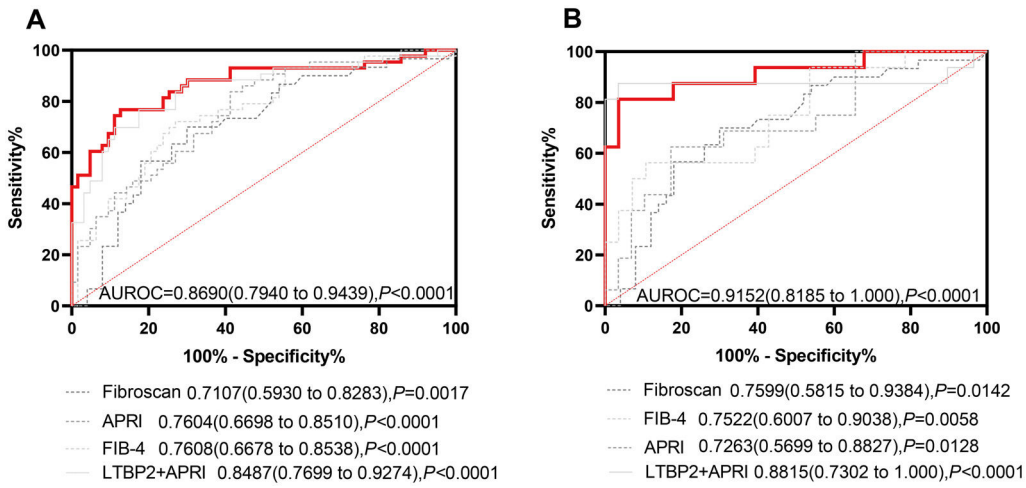

Fig. 7. Receiver operating characteristic curve of the performance of LPA model, APRI, FIB-4, Fibroscan, and LTBP2+APRI in the training cohort and validation cohort. A. ROC curve to assess discrimination performance in the training cohort. B. ROC curve for assessing discrimination performance in the validation cohort. The red lines represent the LPA model.(For interpretation of the references to color in this figure legend, the reader is referred to the web version of this article.)

LTBP2 is a multi-domain exocrine protein present in the ECM. It is an important molecule in the TGF-β complex, participates in forming microfibrils, and plays a role in cell adhesion, belonging to the LTBP fibrin family.

Previous studies have shown that LTBP2 may be associated with fibrosis or tissue remodeling in multiple organs, including the skin [33], heart [34], and lungs [35]. A study of dilated cardiomyopathy (DCM) showed that LTBP2 was upregulated in fibrotic tissues of DCM rats, and silencing LTBP2 reduced oxidative stress damage, myocardial fibrosis, and myocardial remodeling in DCM rats by downregulating the NF-κB signaling pathway [36]. Increased LTBP2 expression was also found in Bleomycin-induced mouse models of pulmonary fibrosis, and silencing LTBP2 prevents fibroblast differentiation into myofibroblasts and subsequent pulmonary fibrosis by inhibiting the phosphorylation of NF-κB signaling and nuclear trans-localization [35]. Studies have shown that LTBP2 expression is upregulated in human thyroid cancer cell lines and that LTBP2 knockdown inhibits the proliferation, invasion, and EMT phenotype of thyroid cancer cells and can reduce thyroid cancer growth in nude mice [37]. Other studies have shown that LTBP2 expression is increased in gastric cancer and that LTBP2 silencing effectively inhibits the proliferation, migration, and epithelial-mesenchymal transformation of gastric cancer cells [38]. In our study, KEGG and GO pathway enrichment analyses revealed that LTBP2 was enriched in collagen-containing ECM and ECM structural constituent pathways. Currently, no study has reported its role and function in LF. Based on our results, we speculate that LTBP2 may be a novel biomarker and therapeutic target for LF. Studies have demonstrated that the MAPK signaling pathway is closely associated with liver fibrosis [39]. TGF-β is a vital activator of the MAPK signaling pathway [40]. Our results reveal that TGF-β upregulates the expression of LTBP2. Whether LTBP2 plays a role in liver fibrosis via the MAPK signaling pathway demands further investigation. This will constitute the focus of our future research on the mechanism of LTBP2 in liver fibrosis.

And there are some limitations to our study. First, although there is little literature showing related influencing factors in the form of nomograms in liver fibrosis, our study cohort is not large enough. These results may not fully summarize the characteristics that affect patient outcomes. Second, all samples were from a single center, and external hospitals other than our hospital could not be used to verify our conclusions. Third, the use of serum markers like LTBP2 has limitations, such as potential interference from other factors that affect liver function. Fourth, further in vivo and in vitro experiments are needed to test the role of LTBP2 in LF therapy.

5. Conclusions

This study suggests that LTBP2 may play a key role in LF development based on whole-genome expression profiles of HBV-associated LF patients combined with HSCs data. It was also identified as an etiologically independent factor in the LF database due to other causes. In addition, our study developed the nomogram model with LTBP2, PLT, and AST as variables to predict the probability of significant fibrosis. The LPA model showed better diagnostic performance in patients and may help clinicians in the future.

Author contributions

M-X L and L C designed the study. All authors were involved in sample collection, generation, collection, compilation and analysis of data. M-X L, S T and X-Y L wrote the manuscript; L C, Y Z and Q L revised the manuscript. All the authors have read the manuscript and approved the final manuscript.

Declaration of interests

None.

Acknowledgments

We thank all the participants in the study.

Funding Information

This study was supported by the ShenKang development center of Shanghai (SHDC12020109), Shanghai Association for Science and Technology (21S11905600) and the Shanghai Municipal Health Commission (2022YQ027).

Data availability Statement

The data presented in this study are available on request from the corresponding author.

Supplementary materials

Supplementary material associated with this article can be found in the online version at doi:10.1016/j.aohep.2024.101744.

References

[1] Friedman SL. Mechanisms of hepatic fibrogenesis. Gastroenterology 2008;134 (6):1655–69. https://doi.org/10.1053/j.gastro.2008.03.003.

[2] Barry AE, Baldeosingh R, Lamm R, Patel K, Zhang K, Dominguez DA, et al. Hepatic stellate cells and hepatocarcinogenesis. Front Cell Dev Biol 2020;8:709. https://doi.org/10.3389/fcell.2020.00709.

[3] Sung YC, Liu YC, Chao PH, Chang CC, Jin PR, Lin TT, et al. Combined delivery of sorafenib and a MEK inhibitor using CXCR4-targeted nanoparticles reduces hepatic fibrosis and prevents tumor development. Theranostics 2018;8(4):894–905. https://doi.org/10.7150/thno.21168.

[4] Gäbele E, Brenner DA, Rippe RA. Liver fibrosis: signals leading to the amplification of the fibrogenic hepatic stellate cell. Front Biosci J Virtual Libr 2003;8:d69–77. https://doi.org/10.2741/887.

[5] Taylor RS, Taylor RJ, Bayliss S, Hagström H, Nasr P, Schattenberg JM, et al. Association between fibrosis stage and outcomes of patients with nonalcoholic fatty liver disease: a systematic review and meta-analysis. Gastroenterology 2020;158 (6):1611–25 e12. https://doi.org/10.1053/j.gastro.2020.01.043.

[6] Cheuk-Fung Yip T, Fan JG, Wai-Sun Wong V. China's fatty liver crisis: a looming public health emergency. Gastroenterology 2023. https://doi.org/10.1053/j.gastro.2023.06.008.

[7] Bedossa P, Carrat F. Liver biopsy: the best, not the gold standard. J Hepatol 2009;50(1):1–3. https://doi.org/10.1016/j.jhep.2008.10.014.

[8] Aydın MM, Akçalı KC. Liver fibrosis. Turk J Gastroenterol Off J Turk Soc Gastroenterol 2018;29(1):14–21. https://doi.org/10.5152/tjg.2018.17330.

[9] Lurie Y, Webb M, Cytter-Kuint R, Shteingart S, Lederkremer GZ. Non-invasive diagnosis of liver fibrosis and cirrhosis. World J Gastroenterol 2015;21 (41):11567–83. https://doi.org/10.3748/wjg.v21.i41.11567.

[10] Sherman KE, Abdel-Hameed EA, Ehman RL, Rouster SD, Campa A, Martinez SS, et al. Validation and refinement of noninvasive methods to assess hepatic fibrosis: magnetic resonance elastography versus enhanced liver fibrosis index. Dig Dis Sci 2020;65(4):1252–7. https://doi.org/10.1007/s10620-019-05815-z.

[11] Liaw YF, Leung N, Kao JH, Piratvisuth T, Gane E, Han KH, et al. Asian-Pacific consensus statement on the management of chronic hepatitis B: a 2008 update. Hepatol Int 2008;2(3):263–83. https://doi.org/10.1007/s12072-008-9080-3.

[12] Desmet VJ, Gerber M, Hoofnagle JH, Manns M, Scheuer PJ. Classification of chronic hepatitis: diagnosis, grading and staging. Hepatol (Baltimore, Md) 1994;19 (6):1513–20.

[13] Goodman ZD. Grading and staging systems for inflammation and fibrosis in chronic liver diseases. J Hepatol 2007;47(4):598–607. https://doi.org/10.1016/j.jhep.2007.07.006.

[14] Chinese society of hepatology CMACSoG, Chinese medical association; chinese society of infectious diseases, chinese medical association. Consensus on the diagnosis and treatment of hepatic fibrosis (2019). J Dig Dis 2020;21(3):127–38. https://doi.org/10.1111/1751-2980.12854.

[15] Sterling RK, Lissen E, Clumeck N, Sola R, Correa MC, Montaner J, et al. Development of a simple noninvasive index to predict significant fibrosis in patients with HIV/HCV coinfection. Hepatology (Baltimore, Md) 2006;43(6):1317–25. https://doi.org/10.1002/hep.21178.

[16] Vallet-Pichard A, Mallet V, Nalpas B, Verkarre V, Nalpas A, Dhalluin-Venier V, et al. FIB-4: an inexpensive and accurate marker of fibrosis in HCV infection. comparison with liver biopsy and fibrotest. Hepatology (Baltimore, Md) 2007;46(1):32–6. https://doi.org/10.1002/hep.21669.

[17] Schuppan D, Afdhal NH. Liver cirrhosis. Lancet 2008;371(9615):838–51. https://doi.org/10.1016/s0140-6736(08)60383-9.

[18] Lin CY, Chin CH, Wu HH, Chen SH, Ho CW, Ko MT. Hubba: hub objects analyzer—a framework of interactome hubs identification for network biology. Nucleic Acids Res 2008;36:W438–43 Web Server issue. https://doi.org/10.1093/nar/gkn257.

[19] Shannon P, Markiel A, Ozier O, Baliga NS, Wang JT, Ramage D, et al. Cytoscape: a software environment for integrated models of biomolecular interaction networks. Genome Res 2003;13(11):2498–504. https://doi.org/10.1101/gr.1239303.

[20] Wang M, Gong Q, Zhang J, Chen L, Zhang Z, Lu L, et al. Characterization of gene expression profiles in HBV-related liver fibrosis patients and identification of ITGBL1 as a key regulator of fibrogenesis. Sci Rep 2017;7:43446. https://doi.org/10.1038/srep43446.

[21] El Taghdouini A, Najimi M, Sancho-Bru P, Sokal E, van Grunsven LA. In vitro reversion of activated primary human hepatic stellate cells. Fibrogenesis Tissue Repair 2015;8:14. https://doi.org/10.1186/s13069-015-0031-z.

[22] Yang A, Yan X, Fan X, Shi Y, Huang T, Li W, et al. Hepatic stellate cells-specific LOXL1 deficiency abrogates hepatic inflammation, fibrosis, and corrects lipid metabolic abnormalities in non-obese NASH mice. Hepatol Int 2021;15(5):1122–35. https://doi.org/10.1007/s12072-021-10210-w.

[23] Gerhard GS, Hanson A, Wilhelmsen D, Piras IS, Still CD, Chu X, et al. AEBP1 expression increases with severity of fibrosis in NASH and is regulated by glucose, palmitate, and miR-372-3p. PLoS ONE 2019;14(7):e0219764. https://doi.org/10.1371/journal.pone.0219764.

[24] Teratani T, Tomita K, Suzuki T, Furuhashi H, Irie R, Nishikawa M, et al. Aortic carboxypeptidase-like protein, a WNT ligand, exacerbates nonalcoholic steatohepatitis. J Clin Invest 2018;128(4):1581–96. https://doi.org/10.1172/jci92863.

[25] Kimura T, Iwadare T, Wakabayashi SI, Kuldeep S, Nakajima T, Yamazaki T, et al. Thrombospondin 2 is a key determinant of fibrogenesis in non-alcoholic fatty liver disease. Liver Int: Off J Int Assoc Study Liver 2024;44(2):483–96. https://doi.org/10.1111/liv.15792.

[26] Kozumi K, Kodama T, Murai H, Sakane S, Govaere O, Cockell S, et al. Transcriptomics identify thrombospondin-2 as a biomarker for NASH and advanced liver fibrosis. Hepatology (Baltimore, Md) 2021;74(5):2452–66. https://doi.org/10.1002/hep.31995.

[27] Hu T, Wang S, Huang L, Wang J, Shi D, Li Y, et al. A clinical-radiomics nomogram for the preoperative prediction of lung metastasis in colorectal cancer patients with indeterminate pulmonary nodules. Eur Radiol 2019;29(1):439–49. https://doi.org/10.1007/s00330-018-5539-3.

[28] Parsons CJ, Takashima M, Rippe RA. Molecular mechanisms of hepatic fibrogenesis. J Gastroenterol Hepatol 2007 22 Suppl 1:S79-84. https://doi.org/10.1111/j.1440-1746.2006.04659.x.

[29] Chen W, Yang A, Jia J, Popov YV, Schuppan D, You H. Lysyl oxidase (LOX) family members: rationale and their potential as therapeutic targets for liver fibrosis. Hepatology (Baltimore, Md) 2020;72(2):729–41. https://doi.org/10.1002/hep.31236.

[30] Ro HS, Kim SW, Wu D, Webber C, Nicholson TE. Gene structure and expression of the mouse adipocyte enhancer-binding protein. Gene 2001;280(1–2):123–33. https://doi.org/10.1016/s0378-1119(01)00771-5.

[31] Tumelty KE, Smith BD, Nugent MA, Layne MD. Aortic carboxypeptidase-like protein (ACLP) enhances lung myofibroblast differentiation through transforming growth factor β receptor-dependent and -independent pathways. J Biol Chem 2014;289(5):2526–36. https://doi.org/10.1074/jbc.M113.502617.

[32] Liu N, Liu D, Cao S, Lei J. Silencing of adipocyte enhancer-binding protein 1 (AEBP1) alleviates renal fibrosis in vivo and in vitro via inhibition of the β-catenin signaling pathway. Hum Cell 2023;36(3):972–86. https://doi.org/10.1007/s13577-023-00859-w.

[33] Sideek MA, Teia A, Kopecki Z, Cowin AJ, Gibson MA. Co-localization of LTBP-2 with FGF-2 in fibrotic human keloid and hypertrophic scar. J Mol Histol 2016;47 (1):35–45. https://doi.org/10.1007/s10735-015-9645-0.

[34] Shi C, Li X, Hong F, Wang X, Jiang T, Sun B, et al. Latent-transforming growth factor β-binding protein 2 accelerates cardiac fibroblast apoptosis by regulating the expression and activity of caspase-3. Exp Ther Med 2021;22(4):1146. https://doi.org/10.3892/etm.2021.10580.

[35] Zou M, Zou J, Hu X, Zheng W, Zhang M, Cheng Z. Latent transforming growth factor-β binding protein-2 regulates lung fibroblast-to-myofibroblast differentiation in pulmonary fibrosis via NF-κB signaling. Front Pharmacol 2021;12:788714. https://doi.org/10.3389/fphar.2021.788714.

[36] Pang XF, Lin X, Du JJ, Zeng DY. LTBP2 knockdown by siRNA reverses myocardial oxidative stress injury, fibrosis and remodelling during dilated cardiomyopathy. Acta Physiol (Oxf) 2020;228(3):e13377. https://doi.org/10.1111/apha.13377.

[37] Wan F, Peng L, Zhu C, Zhang X, Chen F, Liu T. Knockdown of latent transforming growth factor-β (TGF-β)-binding protein 2 (LTBP2) inhibits invasion and tumorigenesis in thyroid carcinoma cells. Oncol Res 2017;25(4):503–10. https://doi.org/10.3727/096504016x14755368915591.

[38] Wang J, Liang WJ, Min GT, Wang HP, Chen W, Yao N. LTBP2 promotes the migration and invasion of gastric cancer cells and predicts poor outcome of patients with gastric cancer. Int J Oncol 2018;52(6):1886–98. https://doi.org/10.3892/ijo.2018.4356.

[39] Liu N, Feng J, Lu X, Yao Z, Liu Q, Lv Y, et al. Isorhamnetin inhibits liver fibrosis by reducing autophagy and inhibiting extracellular matrix formation via the TGF-β1/Smad3 and TGF-β1/p38 MAPK pathways. Mediat Inflamm 2019;2019: 6175091. https://doi.org/10.1155/2019/6175091.

[40] Dewidar B, Meyer C, Dooley S, Meindl-Beinker AN. TGF-β in hepatic stellate cell activation and liver fibrogenesis-updated 2019. Cells 2019;8(11):1419. https://doi.org/10.3390/cells8111419.